CYCLOTRON SPECTRAL INTENSITIES FROM AM-HER SYSTEMS

Ali M Qudah

Phys. Dept., Mu'tah University, Mu'tah, Al-Karak, Jordan

Abstract

The ordinary and extraordinary uncoupled Cyclotron radiation mode intensities, I_+ and I_- respectively, are being calculated for radiative accretion shocks onto magnetic binary AM-Her systems. The calculation is being performed for accretion onto a primary white dwarf star having a 0.3 solar mass; radius $R_* = 1.23 \times 10^9$ cm. The calculation corresponds to the accretion rate $L_{acc} = 3.2 \times 10^{-3} L_{Edd}$. Here L_{Edd} is the Eddington accretion luminosity. At a given instant of time, variation of both modes intensities with harmonic numbers is investigated for various angles of observation. This is done for on axis accretion; where the geometric factor $a_0 = 500$. The field on the pole is taken to be $B_* = 12$ MG. Also for a certain direction and harmonic number, the time dependent intensities are being calculated for various fields; $B_* = 15, 17, 23$ MG.

Keywords: Shock waves, Accretion, Binaries, Magnetic white dwarfs, Cyclotron radiation

Introduction

Magnetic CVs (AM-Her systems) are semi-detached binary systems consisting of a secondary normal late-type red dwarf companion donor; transfering matter to a compact strongly magnetic accreting white dwarf primary star (Patterson 1984; Smith and Dihllon 1998; Liebert and Stockman 1985; Cropper 1990; Mennickent and Diaz 2002; Katysheva and Pavlenko 2003; Littlefair et al. 2003). For a thorough review of CVs, see Warner (1995). The strong magnetic field of the primary usually synchronizes the white dwarf spin to the orbital period (Mukai et al. 2003). The magnetic white dwarf primary acts like a particle accelerator. Electrons and ions of the fully ionized plasma in the preshock region spiral out along broken magnetic field lines and accrete directly onto the magnetic white dwarf along

narrow accretion funnels; where the strong magnetic field of the white dwarf (10-100 MG) does not allow the formation of an accretion disk (Chanmugam and Wagner 1977, 1978; Stockman et al. 1977; Katysheva and Pavlenko 2003; Hessman et al. 1997). Some of the AM-Her systems (or Polars) contain highly magnetic white dwarfs with field strengths of (6-240 MG) (Warner 1995). Up to the year 1999, more than 80% of the ~ 65 known polars were discovered in the ROSAT All-Sky Survey (RASS; Voges et al. 1999), with typical count rates for 15^{th} -19^{th} optical magnitudes in the range of 0.2-2.5 counts s^{-1} (Beuermann and Burwitz 1995). The selection criteria of high X-ray count rate and strong optical emission lines resulted in the discovery of polars in the intermediate-to-high accretion rate regimes (Szkody et al. 2003).

Among the many products of the Sloan Digital Sky Survey (York et al. 2000; Stoughton et al. 2002) will be thousands of new white dwarfs extending to fainter than 20^{th} magnitude and distances greater than 1 kpc.

At intermediate accretion rates (1 gm cm^{-2} s^{-1}), a strong standoff (standing) shock is formed above the surface, and the shocked gas cools mainly by 10-30 keV bremsstrahlung emission (Szkody et al. 2003; Mukai et al. 2003). The bulk of emission from the magnetic white dwarf primary is presumably produced in strong shocks; formed as the plasma merges onto the magnetic white dwarf, whose surface acts as lower boundary cold stationary wall for the shock region (Aizu 1973; Somova, Somova, and Najdenov 1998; Wu and Cropper 2001). The accretion shock is formed near the white dwarf surface when the supersonicly accreting plasma becomes subsonic, and is thereby driven to oscillate with a typical oscillation times-cale similar to the cooling time-scale of the shock-heated plasma. The formed shocks are observed to emit hard x-rays and strongly polarized cyclotron optical emission, both of which are modulated on the orbital period (Cropper 1990, Somova, Somova, and Najdenov 1998). The orbital separation of the binaries is small; that the radius of the normal star exceeds its Roche lobe, and thus loses mass through the inner lagrangian point to the compact magnetic white dwarf primary star (Watson and Dhillon 2001). These studies stimulated searches for fast photometric variabilities in accreting magnetic white dwarfs and led to the discovery of optical quasi-periodic-oscillations (QPOs); for example in the AM-Herculis systems: V834 Cen, AN UMa, EF Eri, VV Pup and BL Hydri (Middleditch 1982, Mason et al. 1983, Larsson 1985, 1987; Middleditch et al. 1991; Ramseyer et al. 1993; Beardmore et al. 1997; Middleditch et al. 1997; Wolff et al. 1999). For steady gas accretion at a rate $\dot{M}$ onto a magnetic white dwarf star of mass M_* and radius R_*, the accretion luminosity is

$$L_{acc} = |\Phi g| \dot{M} = \frac{GM_*}{R_*} \dot{M} \qquad (1)$$

The magnitude of the gravitational potential of the magnetic White dwarf is $|\Phi g| \sim 10^{17} - 10^{18}$ erg g^{-1}. For the modest accretion rates, $\dot{M} \sim 10^{14} - 10^{18}$ gm s^{-1}, the calculated luminosities are consistent with those observed.

Magnetic field calculations are based on the interpretation that polarized light is due to cyclotron emission (Chanmugam and Dulk 1981; Meggitt and Wickramasinghe 1982). In some systems, the field strength has been found from Zeeman spectroscopy. AM-Her has B_* = 13 MG (Schmidt, Stockman and Margon 1981; Latham Liebert and Steiner 1981; Patterson and Price 1981; Young, Schneider and Shectman 1981; Hutchings, Crampton and Cowley 1981; Wickramasinghe and Martin 1985; Bailey et al. 1991). In AM Hers (Beuermann and Burwitz 1995): about 12- 14 MG in AM Her itself (Bailey et al. 1991), EF Eri (¨ Ostreicheret al. 1990), and RXJ1957-57 (Thomas., Beuermann, Schwope., Burwitz 1996). The white dwarf in the BL Hyi system is believed to have a relatively weak magnetic field B_* = 12 MG (Schwope et al. 1995; Wolff et al. 1999). ST LMi has B_* = 19 MG (Schmidt, Stockman and Grandi 1983), and V834 Cen has B_* = 22 MG (Beuermann, Thomas and Schwope 1989). V2301 Oph has B_* = 7 MG (Ferrario et al. 1995).

The isolated white dwarf PG 2329+267 has B_* = 23 MG (Moran, Marsh and Dhillion 1998). For RX J0453.4-4213, the analysis of the phase dependent movement of the maxima for Cyclotron harmonics leads to a magnetic field strength in the accretion region of B_* = 36 MG (Burwitz, Reinsch, Schwope, Beuermann, Thomas, and Greiner 1996). Optical studies of AX J2315-592, indicates that the main contribution to optical flux during the bright phase is from optically thin cyclotron emission in a relatively low magnetic field, $B_* < 17$ MG (Thomas and Reinsch 1996). The improved sample statistics and uniformity indicate that the distribution of magnetic white dwarfs has a broad peak in the range ~ 5 – 30 MG (Schmidt and et al. 2003). Cataclysmic variables (CVs) have strong magnetic fields, $B_* \sim$ 10-100 MG (Cropper 1990, Katysheva and Pavlenko 2003). A relatively large number of them have $B_* \sim$ 20-40 MG, which is one of the reasons that motivate the choice of B_* for our calculations.

The centered dipole configuration is able to fit the spectra for some stars. However, some others require longitudinally offset dipoles or even quadrupoles to obtain satisfactory fits (Schmidt et al. 1986). Also some like WD1953-011 have peculiar field structure consisting of a high-field region covering about 10 percent of the surface area of the star, superimposed on an underlying relatively weak dipolar field (Maxted et al. 2000). The

structure and shape of the accretion region, and hence the magnetic field topology, are probably more complicated than typically assumed.

Physical Picture and Numerical Model

The model assumes that a fully-ionized solar-composition-plasma flows from the companion star to the primary magnetic white dwarf star. Plasma flows along presumably dipolar magnetic field lines (Imamura et al. 1991). Thus, the one-fluid, one-dimensional time-dependent hydrodynamic equations are solved for plasma constrained to flow along individual dipolar field lines:

The mass continuity, momentum and energy equations, and equation of state are solved to generate the time-dependent temperature and density structure of the hot post-shock plasma for independently oscillating magnetically confined flux tubes:

Mass continuity equation: $\frac{\partial \rho}{\partial t} + \nabla.(\rho \vec{V}) = 0$ (2)

Equation of motion: $\rho(\frac{\partial}{\partial t} + \vec{V}.\nabla)\vec{V} = -\nabla P - \rho \nabla \Phi_g + \rho F_{rad}$ (3)

Energy equation: $\frac{\partial \rho I}{\partial t} = -P\nabla.\vec{V} - \nabla.(\rho I \vec{V} + \vec{q}_e) - \Lambda$ (4)

Equation-of-state: $P = (\gamma - 1)\rho I$ (5)

The adiabatic index has the value $\gamma = 5/3$.

The oscillating shock cools off via bremsstrahlung, Compton cooling, and cyclotron emission as it settles onto the white dwarf (Imamura & Steiman-Cameron 1998)). The electron volume loss rate; Λ; is a sum of three contributions: The electron-ion and electron-electron bremsstrahlung, and Compton cooling (Kylafis and Lamb 1982).

The electron thermal conductive flux is given by:

$$\vec{q}_e = -K(T_e)\nabla T_e \quad (6)$$

Where the electrons conductive coefficient is

$$K(T_e) = \frac{1.8x10^{-5} T_e^{5/2}}{\ln(1.11x10^{-5}\rho^{-1/2}T_e)} erg/cm.s.K \quad (7)$$

Equations (2) to (7) are solved together using a modified version of SOLASTAR; a semi-implicit Lagrangian numerical code which uses artificial viscosity to model strong flow discontinuities (Ruppel and Cloutman 1975; Cloutman 1980; Imamura et al. 1991). The code performs the hydrodynamic calculations based on the assumption that bremsstrahlung strongly dominates cyclotron cooling, and the later is not capable of damping shock

oscillations. However, for strong fields ~ 50 MG, the cyclotron cooling strongly stabilizes all modes of the shock harmonic oscillation (Saxton, Wu, and Pongracic 1997; Saxton and Wu 1999; Wu et al. 1996), and its effect is even more profound for sufficiently low accretion rates (Lamb and Masters 1979, King and Lasota 1979). Only in the weak cyclotron case one can decouple the radiative transfer equation from the hydrodynamic equations. So the calculations in this work aim at examining the the cyclotron intensities for shocks onto white dwarfs having field values: $B_* = 15, 17, 23\,\mathrm{MG}$, which is typical for most of the magnetic white dwarfs in binary systems.

The first step is to generate the time dependent hydrodynamic structures based on the assumption that bremsstrahlung strongly dominates cyclotron cooling. We choose to study the first overtone (1O) mode because it does not damp, and its period corresponds to the period of QPOs that are suggested to be cyclotron emission associated with the 1O oscillations (Imamura et al. 1991; Rashed 1997). The second step is to use the generated time-dependent structures to solve the radiative transfer problem for the cyclotron emission.

In terms of the spectral intensity, I_ν, the monochromatic energy, E_ν, flowing across an area element of dA located at $\vec{\mathrm{r}}$ in time dt in the solid angle $d\Omega$ about the direction $\hat{\mathrm{S}}$ (Figure 1) in the frequency interval ν to $\nu + \mathrm{d}\nu$ is:

$$d\mathrm{E}_\nu = \mathrm{I}_\nu(\vec{\mathrm{r}}, \hat{\mathrm{S}}, \mathrm{t}) \cos\Psi \,(\mathrm{d}\nu\, \mathrm{d}\Omega\, \mathrm{dA})\, \mathrm{dt} \qquad (8)$$

In cgs-system, the unit of the spectral intensity is $\mathrm{erg\,s^{-1}\cdot cm^{-2}\cdot sr^{-1}\cdot Hz^{-1}}$. Ψ is the angle the line of sight ($\hat{\mathrm{S}}$) makes relative to the normal ($\hat{n}$) to the area element of the slab (Figures 1, 2).

The monochromatic cyclotron intensity from uncoupled radiation modes is determined through a solution of the time-independent, static radiation transport equation for a hot plasma in the limit of large Faraday rotation (Ramaty 1969):

$$\frac{dI_\pm}{d\tau_\pm} = I_\pm - S_\pm \qquad (9)$$

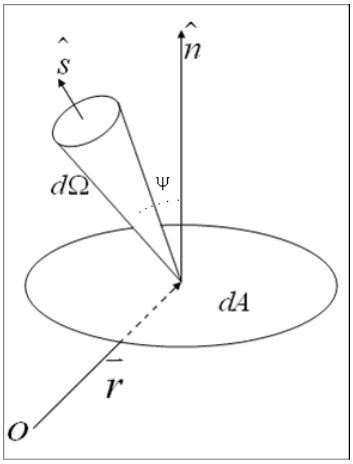

Fig. 1: Flowing across an area element of $\hat{n}\,dA$ in the solid angle $\hat{S}\,d\Omega$, where $\hat{n}$ is the normal to the slab and Ψ is the angle of the line of sight ($\hat{S}$) with respect to $\hat{n}$.

A time-independent formulation for the cyclotron transfer can be used; where the bulk of the emission comes from within an optical depth $\tau_{\pm}=1$, i.e. photons escape essentially unscattered. The optical depth $\tau_{\pm}=-\int\kappa_{\pm}ds$ increases as one goes inward through the accretion funnel. The minus sign is to indicate that optical and geometrical depths increase in opposite directions. Plus and minus signs stand for the ordinary (O) and extraordinary (X) modes; respectively. The Robinson and Melrose formula for the opacity; $\kappa_{\pm}$; is being used (Robinson 1985; and Robinson and Melrose 1984). The optical depths ($\tau_{i,\pm}$) from the surface of the funnel to the exterior surface of the ith. layer is being calculated for the ordinary and extraordinary modes.

For a plasma in local thermodynamic equilibrium, the source function $S_{\pm}$ is given by the local value of the Planck function:

$$S_{\pm}=B(T_i,\nu)=\frac{h\nu^3/c^2}{\exp(\frac{h\nu}{k_BT_i})-1} \qquad (10)$$

Plank function, is calculated for various frequencies and positions across successive layers of the accretion funnel. The ith layer of the funnel is characterized by an average temperature T_i.

The magnetic field is assumed to be dipolar, and its magnitude at position r is

$$B(r,R_*,a_0)=B_0\,(R_*/r)^3\sqrt{[1-3r/(4a_0R_*)}\qquad (11)$$

Here R_* is the radius of the magnetic white dwarf star, B_0 is the magnitude of the field at the polar surface of the star, $a_0 \equiv r_{eq}/R_*$ is a geometrical factor that measures; in units of R_*; the radius r_{eq} at which field lines strike the equatorial plane (Omari et al. 2002). Various values of r_{eq} can be taken, since the cyclotron emission region is seen to extend over a large range in magnetic latitude (Potter et al. 2000).

At surface of the accretion funnel, the solution to the radiative transfer equation gives intensities from uncoupled radiation modes: Ordinary mode intensity I_+ and extraordinary mode intensity I_- according to following expressions

$$I_{\pm}(0,\nu,\mu) = \sum_{i=1}^{n-1} B(T_i,\nu)[\exp(-\tau_{i,\pm}/\mu) - \exp(-\tau_{i+1,\pm}/\mu)] \qquad (12)$$

The time-dependent surface intensity $I_{\pm}(0,\nu,\mu)$ is evaluated for a variety of both photon frequencies ν and direction cosines $\mu = \cos\Psi$ with respect to the magnetic axis i_B, which is almost normal to the slab. The calculations correspond to the narrow funnel (thin ring) accretion region having $a_0 \equiv r_{eq}/R_* = 500$. For several directions and frequencies, the time dependent monochromatic intensities from uncoupled radiation modes are being calculated:

$$I'_{\pm}(r_{eq,i},\Psi,\theta,\nu,t) = I_{\pm}(r_{eq},\theta',\phi',\nu,t)\,\hat{n}.\hat{\Psi} \qquad (13)$$

where $\hat{n}$ is the normal to the slab, and Ψ is the angle of the line of sight ($\hat{S}$) with respect to $\hat{n}$, and θ is the angle of the line of sight relative to polar axis of the star (Figures 1 and 2).

The extended funnel can be thought of as composed of concentric independently oscillating narrow funnels (rings); with each having its own shock structure (Imamura et al. 1991; Ramseyer et al. 1993). Intensities from an extended funnel can be calculated by adding the common frame transformed contributions (i.e. those having matched directions of observations) from all observable parts of the extended funnel to form the resultant intensity: $I_{\pm}(\theta,\nu,t) = \sum_i I'_{\pm}(r_{eq,i},\Psi,\theta,\nu,t)\,\Delta A_i$.

Narrow funnel intensities $I'_{\pm}(r_{eq,i},\Psi,\theta,\nu,t)$ are being calculated for the harmonic numbers $S \equiv \nu/\nu_{cyc} = 1-20$, and for 15 different direction cosines: $(\sqrt{1-\omega^2}, 0, \omega)$. The values of $\omega \equiv \cos\theta$ are presented in Table 1.

Table 1: Fifteen different directions of observation characterized by $\omega = \cos\theta$; the cosine of the angle of the line of sight, $\hat{S}$, relative to polar axis of the star.

Direction	**d1**	**d2**	**d3**	**d4**	**d5**	**d6**	**d7**	**d8**
$\omega = \cos\theta$	0.006	0.0314	0.076	0.138	0.215	0.303	0.399	0.5
Direction	**d9**	**d10**	**d11**	**d12**	**d13**	**d14**	**d15**	
$\omega = \cos\theta$	0.601	0.697	0.786	0.8622	0.924	0.969	0.997	

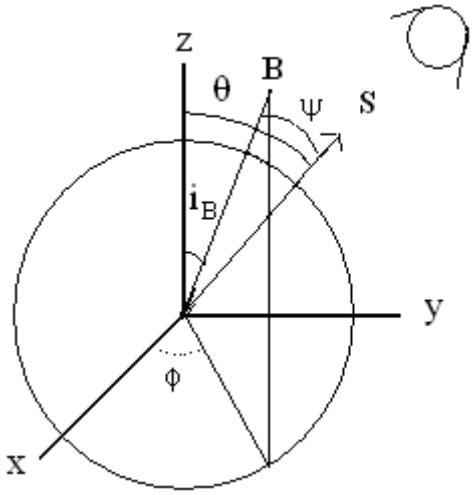

Fig. 2: Directions of observation characterized by $\omega \equiv \cos\theta$; the cosine of the angle of the line of sight, $\hat{S}$, relative to polar axis of the star. Field **B** is normal to the surface of the shock.

Results

The following reults show monochromatic cyclotron spectral intensity from uncoupled radiation modes in units of $\mathrm{erg\,s^{-1}\cdot cm^{-2}\cdot sr^{-1}\cdot Hz^{-1}}$. Figure 3 shows the calculated time dependent ordinary (O) and extraordinary (X) cyclotron intensities; weighted by $\hat{S}.\hat{B}$, for direction cosines: ω = 0.006 (d1), 0.215 (d5), 0.601 (d9). Results correspond to geometric factor $a_0 \equiv 500$, and magnetic field $B_* = 12\,\mathrm{MG}$, and harmonic number S=10.

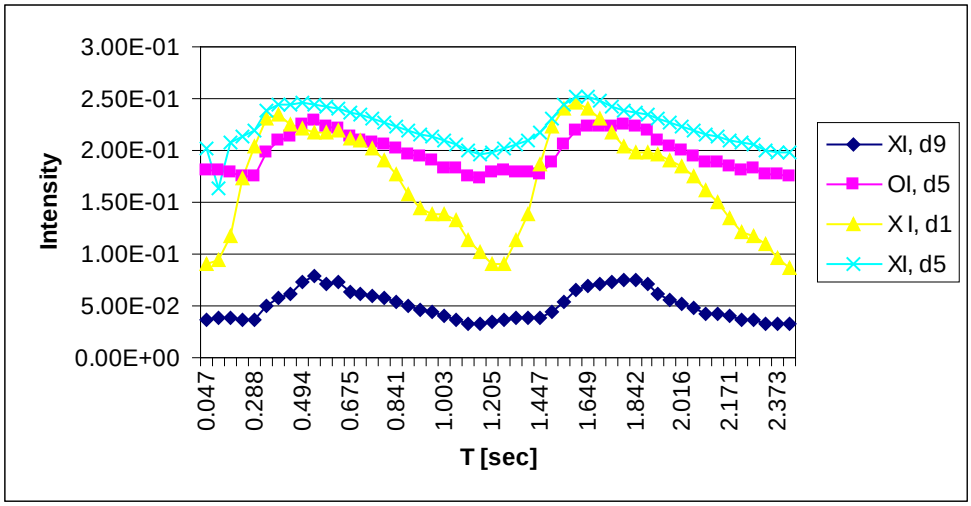

(3-a)

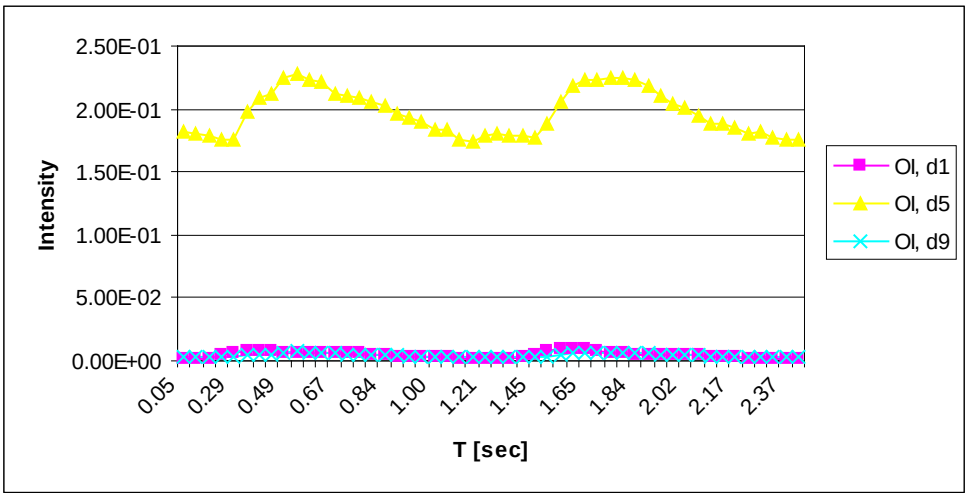

(3-b)

Fig.3: Time dependent ordinary (O) and extraordinary (X) cyclotron intensities; weighted by $\hat{S}.\hat{B}$, for direction cosines: $\omega = \cos\theta$ = 0.006 (d1), 0.215 (d5), 0.601 (d9). Results correspond to $a_0 \equiv 500$, $B_* = 12\,MG$, and harmonic number S=10.

At a given instant of time and for geometric factor $a_0 \equiv 500$, and magnetic field $B_* = 12\,MG$, figures 4-5 show a log-log plot of the calculated cyclotron intensities; weighted by $\hat{S}.\hat{B}$; versus harmonic numbers. Figure **(4-a)** shows the three directions: $\omega = \cos\theta$ = 0.006 (d1), 0.0314 (d2), and 0.076 (d3). While Figure **(4-b)** shows the three directions: ω = 0.138 (d4), 0.215 (d5), and 0.303 (d6). Figure **(5-a)** shows the three directions: ω = 0.399 (d7), 0.5 (d8), and 0.601 (d9). While figure **(5-b)** shows the three directions: ω = 0.697(d10), 0.786 (d11), and 0.8622 (d12).

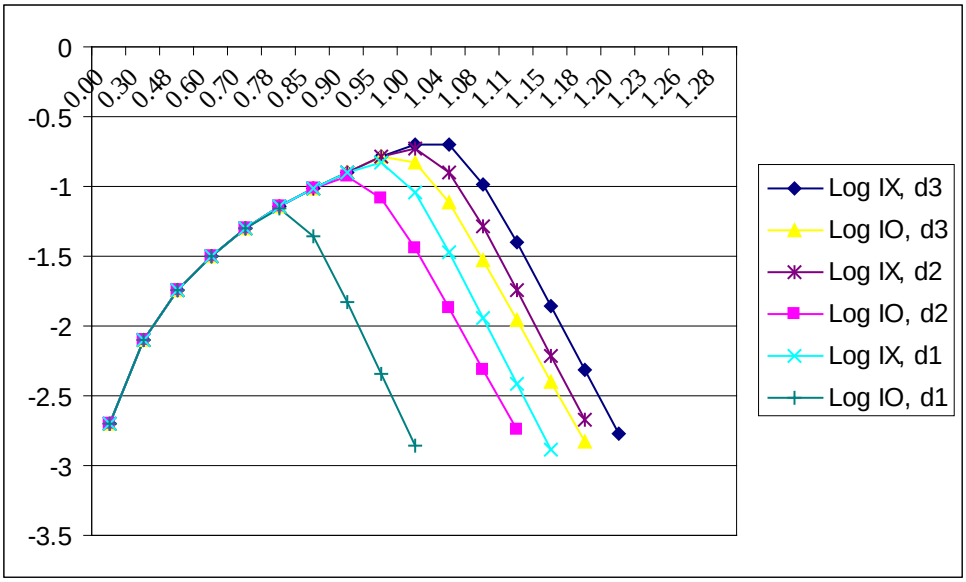

(4-a)

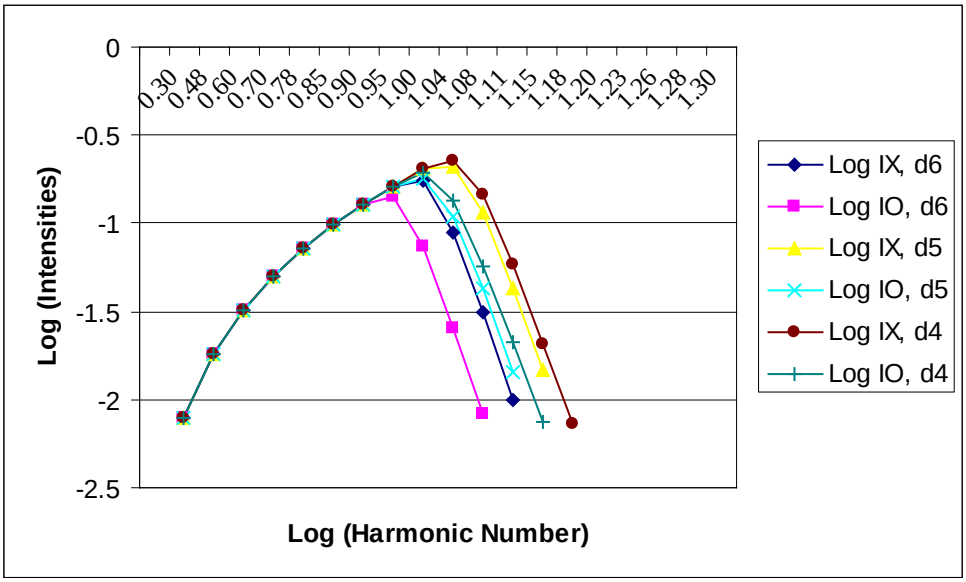

(4-b)

Fig.4: Log cyclotron intensities; weighted by $\hat{S}.\hat{B}$; versus log harmonic numbers at a given instant of time. Results correspond to $a_0 \equiv 500$, $B_* = 12\,MG$. Upper figure **(4-a)** shows the three directions: $\omega = \cos\theta$ = 0.006 (d1), 0.0314 (d2), and 0.076 (d3). While lower figure **(4-b)** shows the three directions: $\omega = \cos\theta$ = 0.138 (d4), 0.215 (d5), and 0.303 (d6).

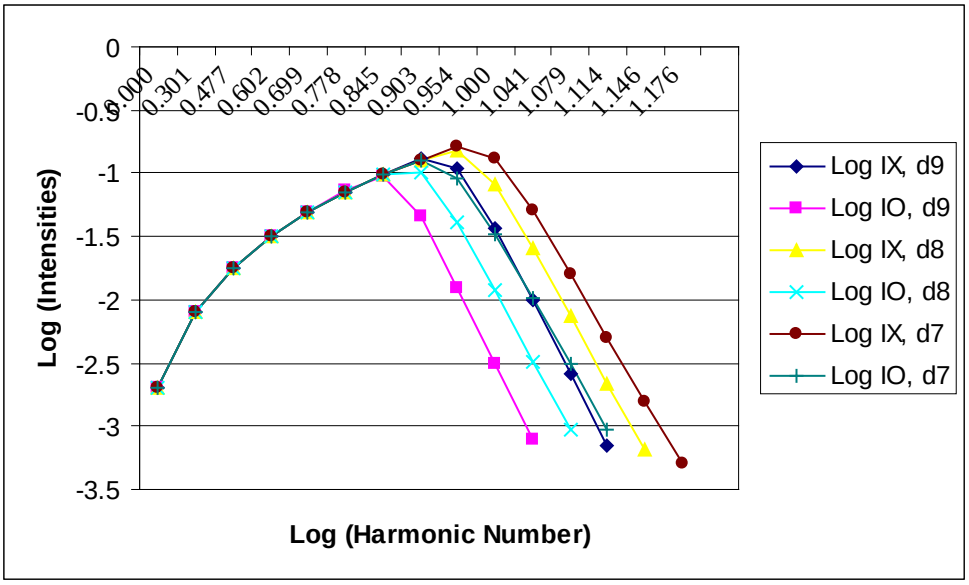

(5-a)

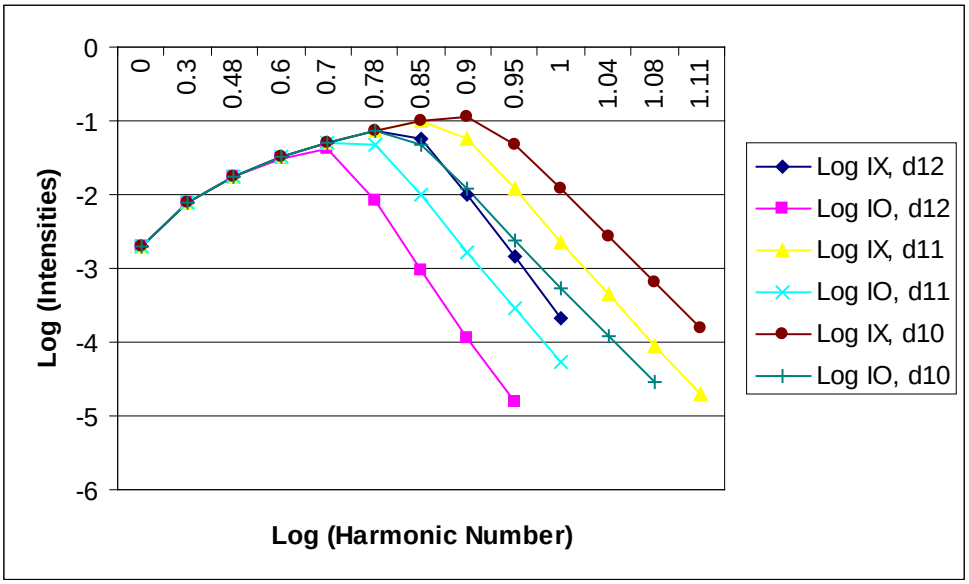

(5-b)

Fig.5: Log cyclotron intensities; weighted by $\hat{S}.\hat{B}$; versus log harmonic numbers at a given instant of time. Results correspond to $a_0 \equiv 500$, $B_* = 12\,\mathrm{MG}$. Figure **(5-a)** shows the three directions: $\omega = \cos\theta$ = 0.399 (d7), 0.5 (d8), and 0.601 (d9). While figure **(5-b)** shows the three directions: $\omega = \cos\theta$ = 0.697(d10), 0.786 (d11), and 0.8622 (d12).

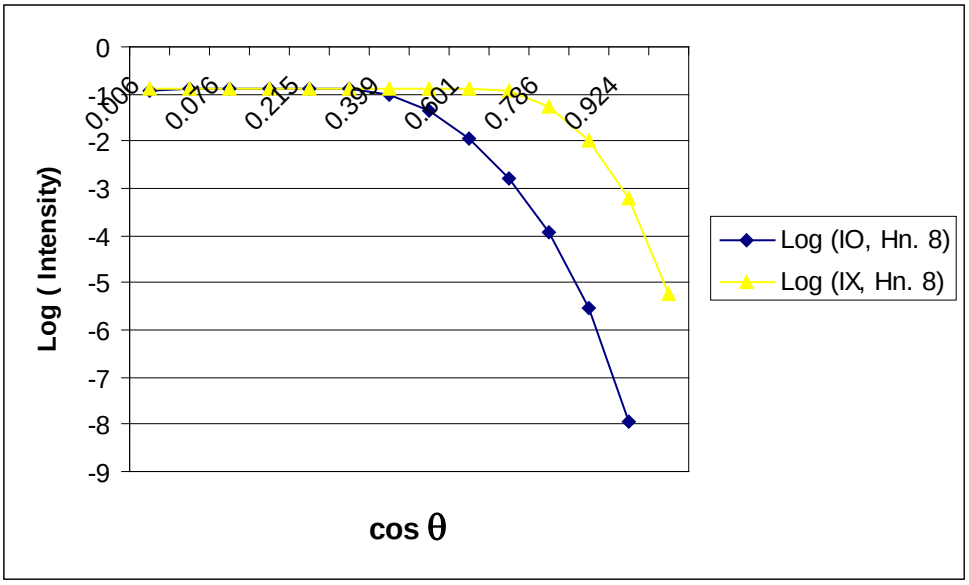

(6-a)

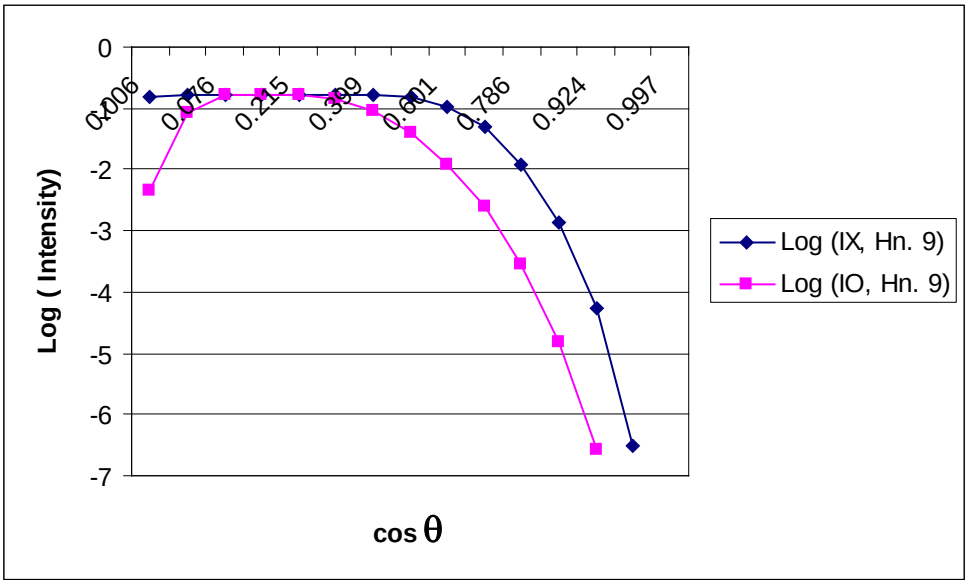

(6-b)

Fig. 6: Log intensity; weighted by $\hat{S}.\hat{B}$; versus $\omega = \cos\theta$. Results correspond to $a_0 \equiv 500$, $B_* = 12\,\mathrm{MG}$. Upper figure for the harmonic number S = 8, and lower figure for the harmonic number S = 9.

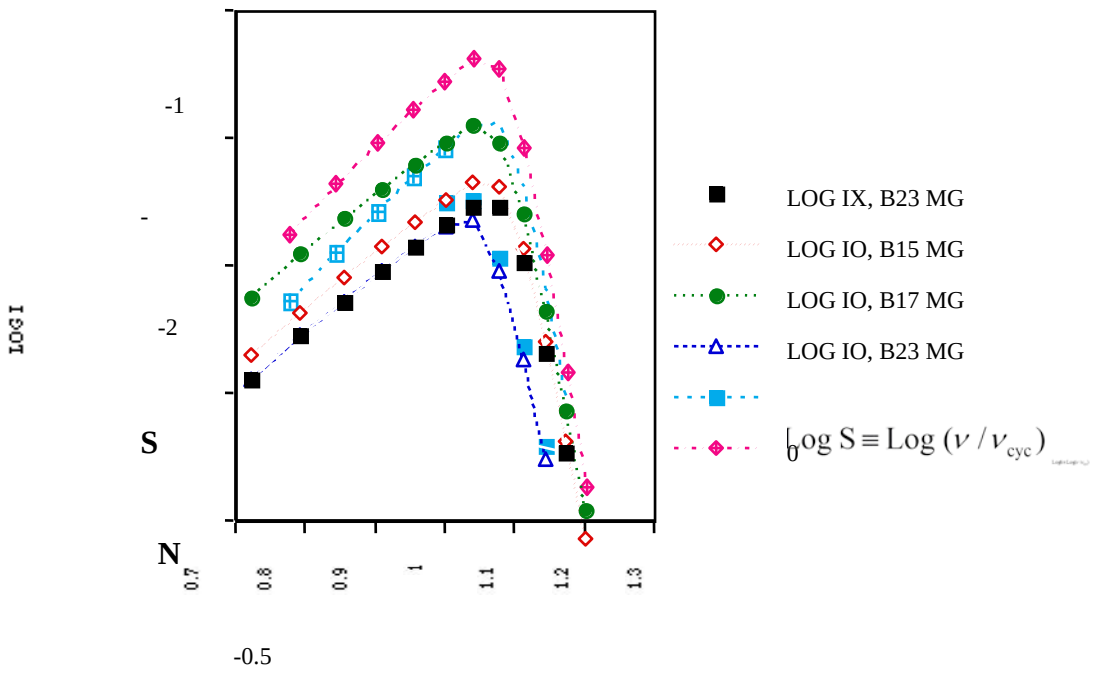

Fig. 7: Log Intensity versus log harmonic number for $\omega = \cos\theta = 0.215$ (d5), $a_0 = 50$, and fields $B_* = 15, 17, 23$ MG .

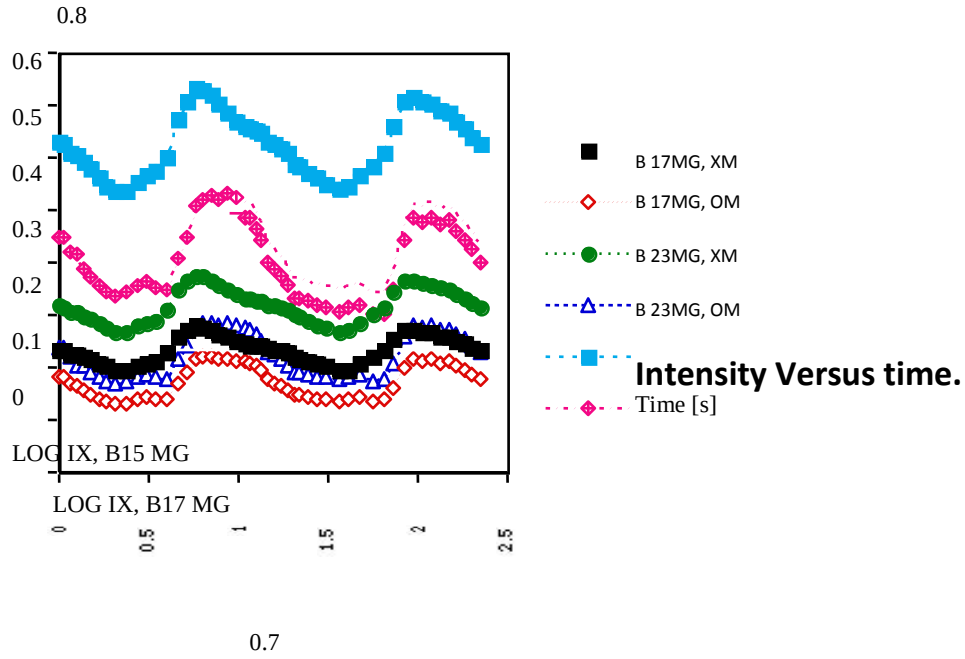

Fig. 8: Ordinary and extraordinary modes intensities versus time for the harmonic S = 9, and direction $\omega = \cos\theta = 0.303$ (d6). $a_0 = 50$, and values of field strength: B = 15, 17, 23 MG.

Discusion and Conclusions

The X mode intensity is larger than the O mode intensity for all the opticaly thin harmonics, and for all directions of observation (Figures 3 - 6). This remains true even as the shock structure varies with time (Figures 3, 8). Also this is true for all values of the magnetic field (Figure 8). Thus, the O mode becomes opticaly thin at a lower harmonic number as

compared to the X mode, which is true for all directions (Figures 4-5). This is also tru for all field values (Figure 7). This is clear from the fact that the O mode peaks at a alower harmonic as compared to the harmonic number corresponding to X mode maximum intensity.

For plasma constrained to flow along a single narrow magnetically confined flux tube, intensities show shoulders and sharp peaks due to areal projection effects. This causes a dip in the spectrum near $\cos\theta = 0$ (Figures 6). This is also due to the decrease in the absorption coefficient in the ordinary mode so that the funnel becomes optically thin as $\cos\theta$ goes to zero, while remaining optically thick in the extraordinary mode. This causes a sharp increase in linear polarization as $\cos\theta$ goes to zero. Due to large area projection effect; $\hat{S}.\hat{B}$ has small value; both modes intensities increase with $\cos\theta$ for the first three directions ($\cos\theta < 0.138$) (Figures: 4-a, 6). While for the remaining directions ($0.138 \le \cos\theta < 1$), both modes intensities are found to stay constant for the optically thick harmonics (Figure: 8), and decrease with $\cos\theta$ for the optically thin harmonics (Figures:4-6, 5, 6). This can be explained as follows: As $\cos\theta$ increases, the funnel becomes optically thick in both modes ($\tau_{\pm} > 1$) and the largest contribution to the intensities is from the shock front which has a higher temperature; $I_{\pm}(0,\nu,\mu) \propto B(T_i,\nu) \propto \nu^2 T_i$. A further increase in $\cos\theta$ makes the ordinary mode optically thin. A further more increase in $\cos\theta$ makes both modes optically thin (but $\tau_{-} >> \tau_{+}$).

Both modes intensities increase mainly with field strength. This is true for all harmonic numbers (Figure 7 and 8), and at all times (Figure 8). This behavior is expected; where in the Rayleigh–Jeans limit, the source function is equal to Planck function: $S_{\pm} = B(T_i,\nu) \cong \nu^2 k_B T_i / c^2$, and the surface intensities, $I_{\pm}(0,\nu,\mu)$, are proportional to $B(T_i,\nu) \propto \nu^2 T_i \propto \nu_{cyc}^2 T_i \propto B^2 T_i$.

References:

Aizu, K., 1973. Prog. Theor. Phys., 49, 1184.

Bailey, J., Ferrario, L., Wickramasinghe, D.T. 1991, MNRAS 251, 37P

Beardmore, A. P.; Osborne, J. P., A GINGA hard X-ray search for 1-3s quasi-periodic oscillations in AM Herculis systems, MNRAS, 1997, 286, Issue 1, pp. 77-80.

Beuermann, K. and Burwitz, V. 1995, in ASP Conf. Ser. 85, Cape Workshop on Magnetic Cataclysmic Variables, ed. D. A. H. Buckley & B. Warner (San Francisco: ASP),99.

Beuermann, K., Thomas, H.-C., and Schwope, A. 1989, IAU Circ., No. 4775. V834 Centauri.

Burwitz V., Reinsch K., Schwope A.D., Beuermann K., Thomas H. C- Greiner, 1996-January(II), Astron. Astrophys., 305, 507-512.

Chanmugam, G. and Dulk, G. A., 1981. ApJ, 244, 569.

Chanmugam, G., Langer, S.H., and shaviv, G., 1985. ApJ, 299, 87.

Chanmugam, G. and Wagner, R. L., The Remarkable System AM Herculis/3U 1809+50. ApJ, 1977. 213, L13. .

Chanmugam, G., and Wagner, R. L., Remarkable System AM Herculis/3U 1809+50. II. A Single accretion Column Model. ApJ, 1978; 222: 641.

Cloutman, L. D., Sola-Star: A One-Dimensional Iced-Ale Hydrodynamic Program For Spherically Symmetric Flows., Los Alamos Scientific Laboratory Report LA-8452-MS., 1980.

Cropper, M. S.1990, Space Science Reviews, 54, 195.

Ferrario, L., Wickramasinghe, D., Bailey, J., Buckley, D. 1995, MN- RAS 273, 17.

Hessman, F.V., Beuermann, K., Burwitz, V., de Martino, D., and Thomas, H.-C. 1997 Astron. Astrophys., 327, 245–251.

Hutchings, J. B., Crampton, D. and Cowley, A. P., 1981, ApJ, 247, 195.

Imamura, J. N., Rashed, H. Y., and Wolff, M. T. 1991, ApJ, 378, 665.

Imamura J. N., Steiman-Cameron T. Y., 1998, ApJ, 501, 830.

Katysheva, N. A. and Pavlenko, E. P. Cataclysmic variables in the "period gap", 2003, Astrophysics, Vol. 46, No. 1, 114.

King, A. R., and Lasota, J. P. 1979, MNRAS, 188, 653

Kylafis, N. D., and Lamb, D. Q. 1982, X-Ray and UV Radiation From Accreting Nonmagnetic Degenerate Dwarfs, ApJ Supp. Ser., 48, 239.

Lamb, D. Q., and Masters, A. R. 1979, ApJ, 234, L117

Latham, D. W., Liebert, J. and Steiner, J. E., 1981. ApJ, 246, 919.

Larsson, S.1985, Astr. Ap., 145, L1.

Larsson, S. 1987, Astr. Ap., 181, L15.

Liebert, J., and Stockman, H. S. 1985, in 7th North American Workshop on Cataclysmic Variables and Low Mass X-Ray Binaries, ed. D. Q. Lamb and J. Patterson (Dordrecht: Reidel), P.151-178.

Littlefair, S. P., Dhillon, V. S., and Martin, E. L. 2003,On the evidence for brown dwarf secondary stars in cataclysmic variables. MNRAS, 340, 264-268.

Mason, K. O., Middleditch, J., Cordova, F. A., Reichert, G., Murdin, P. G., Clarke, D., and Bowyer, S. 1983, ApJ, 264, 575.

Maxted, P.F.L, Ferrario, L., Marsh, T.R., and Wickramasinghe, D. T. 2000, WD 1953-011: A magnetic white dwarf with peculiar field structure. MNRAS, 315, L41-L44.

Meggitt, S. M. A. and Wickramasinghe, D. T., THE POLARIZATION PROPERTIES OF MAGNETIC ACCRETION COLUMNS. 1982. MNRAS, 198, 71.

Mennickent, R. E. and Diaz, M. P., A search for brown dwarf like secondaries in cataclysmic variables, 2002, MNRAS, 336, 767-773.

Middleditch, J. 1982, ApJ, 257, L71.

Middleditch, J., Imamura, J.N., & Steiman-Cameron, T.Y. 1997, ApJ, 489, 912.

Middleditch, John; Imamura, James N.; Wolff, Michael T.; Steiman-Cameron, Thomas, Y., 1991, ApJ, 382, 315.

Moran, C., Marsh, T. R., and Dhillion, V. S. 1998, MNRAS, 299, 28.

Mukai, K. and et al. 2003, ApJ, 597: 479-493.

Omari, H. Y., and et al. 2002, On-Axis large Time Scale Polarization of AM-Her Stars, ABHATH AL-YARMOUK, Basic Sciences and Engineering, vol. 11, No.1B, pp 287-303.

Ostreicher, R., Seifert, W., Wunner, G., Ruder, H. 1990, ApJ 350, 324

Patterson, J. 1984, ApJS, 54, 443.

Patterson, J. and Price, C., 1981. Publ. Astronm. Soc. Pacif., 93, 71.

Potter, S. B., Cropper, M. and Hakala, P. J. 2000, Stokes imaging of the accretion region in magnetic cataclysmic variables. MNRAS, 315, 423-430.

Ramaty, R. Gyrosynchrotron Emission and Absorption in a Magnetoactive Plasma, 1969, ApJ, 158, 753.

Ramseyer, Tod F.; Robinson, Edward L.; Zhang, Erho; Wood, Janet H.; Stiening, Rae F.; A survey for QPOs in AM Herculis stars and a detailed study of the QPOs in an Ursae Majoris; 1993, MNRAS, 260, no. 1, p. 209-220.

Rashed, H. Y. Polarized Emission of AM-Herculis Objects, 1997, ApJ, 484, 341-349.

Robinson, P. A. Gyrocynchrotron Emission: Generalization of Petrosian's Method, 1985, ApJ, 298, 161.

Robinson, P. A. and Melrose, D. B. Gyramagnetic Emission and Absorption: Approximate Formulas of Wide Validity, 1984, Aust. J. Phys., 37, 675

Ruppel, H. M., and Cloutman, L. D. A General Numerical Fluid Dynamics Algorithm For Astrophysical Applications, 1975, Los Alamos Scientific Laboratory Report LA-6149-MS.

Saxton, C. J., Wu, K., and Pongracic, H. 1997, Stability of Accretion Shocks. Astronomical Society of Australia, Volume 14, Number 2.

Saxton C. J., Wu K., 1999, MNRAS, 310, 667.

Schmidt, G. D. and et al.,2003. ApJ, 1101, 1113.

Schmidt, G. D., Stockman, H. S. and Grandi, S. A.,1983. ApJ, 271, 735.

Schmidt, G. D., Stockman, H. S. and Margon, B., 1981. A Direct Measurement of the Magnetic Field In AM-Herculis. ApJ, 243, L157.

Schmidt, G. D., West, S. C., Liebert, J., Green, R. F., and Stockman, H. S.,1986. ApJ, 309, 218.

Smith, D. A. and Dihllon, V. S., 1998. MNRAS, 301, 767.

Somova, N. N., Somova, T. A, and Najdenov, I. D., 1998, Astron. Astrophys., 332, 526-540

Stockman, H. S., Schmidt, G. D., Angel, J. R. P., Liebert, J., Tapia, S. and Beaver, E. A., New Observations and a slow Rotator Model of The X-Ray Binary AM-Herculis. , ApJ, 1977; 217: 815-831.

Stoughton, C., et al. 2002, AJ, 123, 485.

Szkody Paula et al. 2003, ApJ, 2003; 583: 902-906

Thomas, H.-C., Beuermann, K., Schwope, A.D., Burwitz, V. 1996, A&A 313, 833

Thomas H.-C., Reinsch K., 1996, Astron. Astrophys., 315, L1-L4.

Thomas and Reinsch

Voges, W. et al. 1999, A&A, 349,389.

Warner, B. 1995, Cataclysmic Variable Stars. Cambridge univ. Press, Cambridge.

Watson, C. A. and Dhillon, V. S. 2001, Roche tomography of cataclysmic variables. MNRAS, 326, 67-77.

Wickramasinghe, D. T., and Martin, B. 1985, The Magnetic Field of AM-Herculis. MNRAS, 212, 353.

Wolff, M. T., Wood K. S.; Imamura, J. N.; Middleditch, J.; and Steiman-Cameron, T. Y. 1999, ApJ, 526:435-444.

Wu, K. and Cropper, M. 2001, The lower boundary of the accretion column in magnetic cataclysmic variables. MNRAS, 326, 686-694.

Wu K., Pongracic H., Chanmugam G., Shaviv G., 1996, Publ. Astron. Soc. Australia, 13, 93.

York, D. G., et al. 2000, AJ, 120, 1579.

Young, P., Schneider, D. P. and Shectman, S. A. 1981. ApJ, 245, 1043.